DOI: 10.1007/s40684-014-0026-z

Numerical Investigation on Composite Porous Layers in Electroosmotic Flow

Taqi Ahmad Cheema[1], Kyung Won Kim[1], Moon Kyu Kwak[1], Choon Young Lee[1], Gyu Man Kim[1], and Cheol Woo Park[1,#]

1 School of Mechanical Engineering, Kyungpook National University, 1370 Sankyuk-dong, Buk-gu, Deagu, South Korea, 702-701
Corresponding Author / E-mail: chwoopark@knu.ac.kr, TEL: +82-53-950-7569, FAX: +82-53-950-6550

KEYWORDS: Porosity, Wall region, Mass transport, Electroosmotic flow, Composite porous layer

Applying mechanical pressure on a solid boundary contact using a thin porous layer has been found to reduce the pore size and porosity near the wall region, limiting the flow and mass transport properties. This reduction may affect the overall performance of devices such as the electroosmotic pump that generally uses a porous media with constant porosity in an electric field. Therefore, to improve the performance of such devices, a composite porous layer that uses a combination of different porosity value based on the location in the porous domain, is employed with a higher porosity near the wall region than that in the central region. In this study, a numerical simulation is conducted to investigate the fluid dynamic and mass transport characteristics using a composite porous layer with electroosmotic flow. A comparison of the results with the pressure-driven flow shows the effectiveness of the composite porous layer in compensating for the loss of porosity and in improving device performance. The proposed methodology may also enhance the performance of green energy devices such as fuel cells.

Manuscript received: March 25, 2014 / Revised: May 16, 2014 / Accepted: May 17, 2014

NOMENCLATURE

c = Concentration of tracer (mol/m^3)
D = Diffusion coefficient (m^2/s)
p = Pressure of fluid (Pa)
$\vec{N}$ = Flux Vector
$\vec{u}$ = Fluid velocity vector (m/s)
$\vec{i}$ = Current density (A/m^2)
z = Tracer charge number
F = Faraday's constant (C/mol)
ρ = Density of fluid (kg/m^3)
μ = Viscosity of fluid (Pa-s)
ε_p = Base porosity of porous layer
ε_w = Fluid permittivity (F/m)
ζ = Zeta potential (V)
τ = Tortuosity of the porous media
a = Average pore radius (m)
κ = Conductivity (S/m)
c_{top} = Peak concentration (mol/m^3)
σ = Base width of peak concentration (m)

1. Introduction

Electroosmotic flow (EOF) is the bulk motion of a liquid across a fluid conduit as a result of the interaction between charged surfaces, ionic solutions and electric fields. The charged surfaces attract the counter ions and repel the co-ions of the solution in contact, forming an electric double layer in the vicinity of the wall.[1] EOF has been previously employed in electrochemistry, physics and vascular plant biology. A number of numerical and experimental investigations on EOF in porous media have been conducted.[2-5] EOF is an attractive choice for engineers and technologists for pumping the fluid through small channels and porous membrane materials without the use of mechanical moving parts. Thus, porous electroosmotic pumps have attained considerable attention in the last decade. Electroosmotic pump is a device that uses a porous membrane to exchange selective ions by EOF and is potentially used for drug delivery, cooling of microelectronic systems and water management in fuel cells.[6-8] In many applications, EOF through porous media is treated as a flow through a large number of parallel tortuous microchannels.[9]

The technological advancement and the importance of porous media in a variety of industrial applications have made it a prominent research

topic for the last three decades. The focus of previous research has been mainly on the development of theories related to porous media but this focus has shifted recently to the performance enhancement of porous media applications. Porosity, permeability, morphological and geometrical configurations are some of the variables considered in former analyses to improve the performance of porous media.[10,11] Numerous experimental and numerical studies on different types of electroosmotic pumps have been conducted, all of which have used a constant porosity and a constant pore diameter.[12,13]

Regarding the pressure-driven flows, the solid boundary contact with porous media has been found to limit flow and mass transfer properties and to affect the overall device performance. Moreover, the application of pressure during the assembly of devices containing thin porous media reduces pore diameter and subsequently the porosity near the wall region.[14,15] In addition, thin porous layers deformed by fluid load also contribute to the reduction of porosity.[16,17] Thus, many previous researchers had focused on variable porosity to address the above-mentioned concerns. However, these investigations had considered the pressure gradient as the only flow-driving force.[18-20] So far the authors' knowledge, the effects of variable porosity with an applied electric field have not been studied, and previous studies have relied only on constant porosity.

The primary objective of the present study is to numerically investigate the EOF in a composite porous layer with an aim to reduce the flow resistance, especially in the near wall region. The void fraction of the porous media is defined by a position based combination of porosity to counter and compensate the reduced porosity because of solid boundary contact and application of mechanical pressure. The proposed composite porous layer makes use of a high porosity value in the outer region rather than in the central region. The effects of this new method of composite porosity on the EOF and mass transport characteristics are investigated by performing a numerical simulation on a 2D composite porous model. At first, the physics of EOF was simulated by solving the conservation equations for flow and current density. The results of this study were then coupled to transient simulation to evaluate the effects of the composite porous layer on specie transport. All results obtained by EOF were compared with the pressure-driven flow in similar conditions. The use of the proposed composite porous layer is advantageous because it enhances fluid and mass transport, without increasing the electric potential. Therefore, the use of a composite porous layer is energy efficient and can be used in green energy devices, such as fuel cells, to compensate for the loss of porosity and to improve the device performance.

2. Model Development and Mathematical Modeling

Generally, the orientation of the porous media is normal to the EOF, as can be observed in an electroosmotic pump. A simple 2D rectangular porous channel connected to two electrodes at the top and bottom corners is shown in Fig. 1. The cross section of the channel is 4 mm × 1.5 mm and is divided vertically into three major domains to implement the concept of a composite porous layer. The porous media was divided based on the boundary layer developed in the same porous layer with constant unit porosity. The outer region was assigned with a higher porosity ($\varepsilon = 0.7$, 0.8 and 0.9) than that in the central region ($\varepsilon = 0.6$).

The computational domain was assumed to contain a single-phase fluid of density 1000 kg/m^3 and viscosity of 1.0 E-03 Pa-s. The effects of electrochemical reaction, compressibility and gravitation had been ignored and a laminar fluid flow was considered. The flow field was investigated using the continuity equation for flow and current density.

$$\nabla.\vec{u} = 0 \tag{1}$$

$$\nabla.\vec{i} = 0 \tag{2}$$

Velocity can be evaluated by the pressure gradient or potential difference according to the following relation:

$$\vec{u} = \left(-\frac{\varepsilon_p a^2}{8\mu\tau}\right)\nabla p + \frac{\varepsilon_p \varepsilon_w \zeta}{\mu\tau}\nabla V \tag{3}$$

Similarly, the current density can be evaluated by using the following relation:

$$\vec{i} = -\kappa\nabla V \tag{4}$$

For the pressure-driven flow, the inlet was introduced with a pressure of 1 kPa, while the outlet boundary conditions were fixed to atmospheric boundary conditions. The walls of the channel domain had no-slip boundary condition. For EOF, all boundaries were assigned with an insulated condition except the electrodes with 50 V and 0 V at anode and cathode surfaces, respectively.

Tracer specie was injected into the channel to investigate the effects of the transient mass transport in the composite porous layer, with the assumption that the specie does not influence the porous structure. Mass transport is governed by the following equation:

$$\frac{\partial c}{\partial t} + \nabla.\vec{N} = 0 \tag{5}$$

where c is the tracer concentration and $\vec{N}$ is the flux vector that can be defined by the Nernst–Planck equation.

$$\vec{N} = -D\nabla c - z u_m F c \nabla V + c\vec{u} \tag{6}$$

where u_m denotes the tracer ion mobility (mol-m^2/J.s) and can be evaluated by using Nernst Einstein equation:

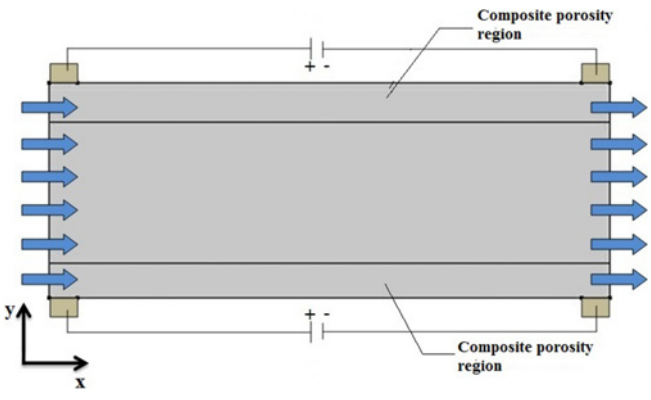

Fig. 1 Porous domain model used for computation

$$u_m = \frac{D}{RT} \tag{7}$$

The inlet and outlet of the channel were assigned flux conditions to set the diffusion and convection contribution. The walls of the porous media were set with symmetry boundary conditions. The initial concentration along the x-axis is given by the following distribution:

$$c(t=0) = c_{top}\exp\left(-0.5\left(\frac{(x-x_m)}{\sigma}\right)^2\right) \tag{8}$$

3. Numerical Method and Implementation

We used the commercial software COMSOL-Multiphysics, which uses a finite element method, to solve discretized equations. The two new slots introduced outside the central region were assigned with higher porosity, ranging from 0.7 to 0.9, than that in the central region that has a base porosity of 0.6. In the first part of the simulation, the two distinct physics of EOF and pressure-driven flow in the porous channel were coupled for a steady-state simulation by a PDE equation solver application mode available in the commercial code. The values of some important parameters used in this study are listed in Table 1.

The computational domain was discretized using triangular mesh with maximum element size of 0.1 mm to form 1,538 elements and 6,378 degrees of freedom were solved. In each case, direct solver was used for 1,000 iterations, with a tolerance factor of 1E-3. In the second stage of the study, a time-dependent numerical simulation was implemented to investigate the species concentration using the steady-state velocity field from the first stage. The solution ran for 1 second, with an interval of 0.1 second, in each geometrical configuration and porosity value.

4. Results and Discussion

4.1 Effect on Electroosmotic Flow (EOF) Velocity

Fig. 2 shows the EOF velocity surface plots, with arrows showing the direction of the flow in the four cases of porosity. Moreover, the contour lines represent the voltage potential distribution in the fluid domain. The figure clearly indicates that as porosity near the wall region increases, the flow rate in that region increases. However, the effect of this increase in the central region is small at the interface of the two regions, which can be of significant amount if the domain is scaled down to micro level. This kind of increase can eventually enhance device performance in which such combinations of porosity are introduced. From the results, the increase is shown to potentially compensate for the effects of reduction in porosity because of the application of external pressure and solid boundary contact.

Table 1 Parameters used in the simulation

Avg. Pore radius (a)	10 μm
Diffusion Co-efficient (D)	1E-09 m^2/s
Electrical Conductivity (k)	3.4E-5 S/m
Zeta potential (ζ)	-0.1 V
Concentration profile peak width (σ)	0.2 mm
Concentration profile peak position (x_m)	1 mm
Tracer ion charge number (z)	1
Temperature (T)	298 K

The visualized plots of Fig. 2(c), (d) clearly show that electroosmotic velocity increased in the central region that has constant porosity, the difference in porosity is high in the two distinct regions. The absence of viscous and wall shear effects results in a uniform velocity profile in EOF. However, relatively smaller pore

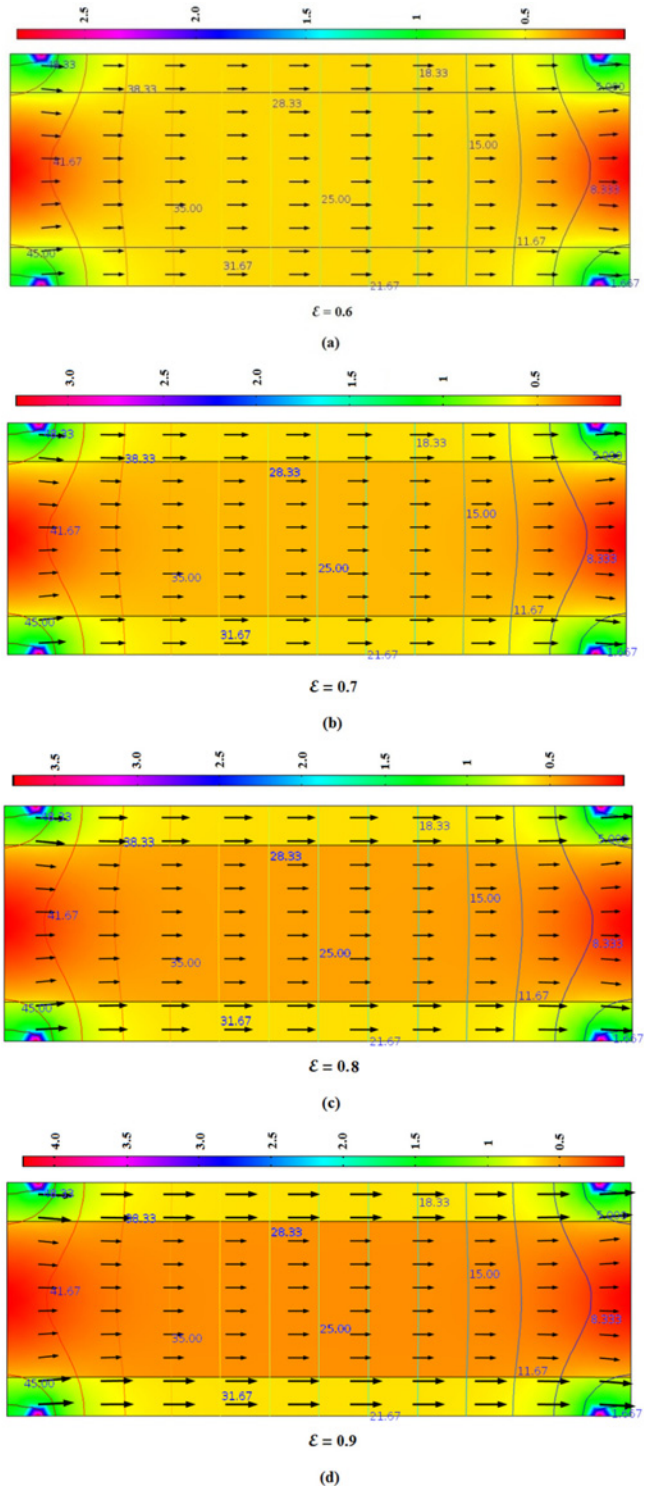

Fig. 2 Effect of composite porosity on electroosmotic velocity magnitude in mm/s (surface plot); voltage potential in V (contour plot) and flow velocity field (arrow plot) for (a) porosity = 0.6, (b) porosity = 0.7, (c) porosity = 0.8 and (d) porosity = 0.9

sizes near the wall region may restrict the velocity field to feature a complete uniform flow. The proposed composite porous layer has solved this issue to some extent, and pumping the fluid in energy devices with the same electric potential such as fuel cells, can be more efficient.[21]

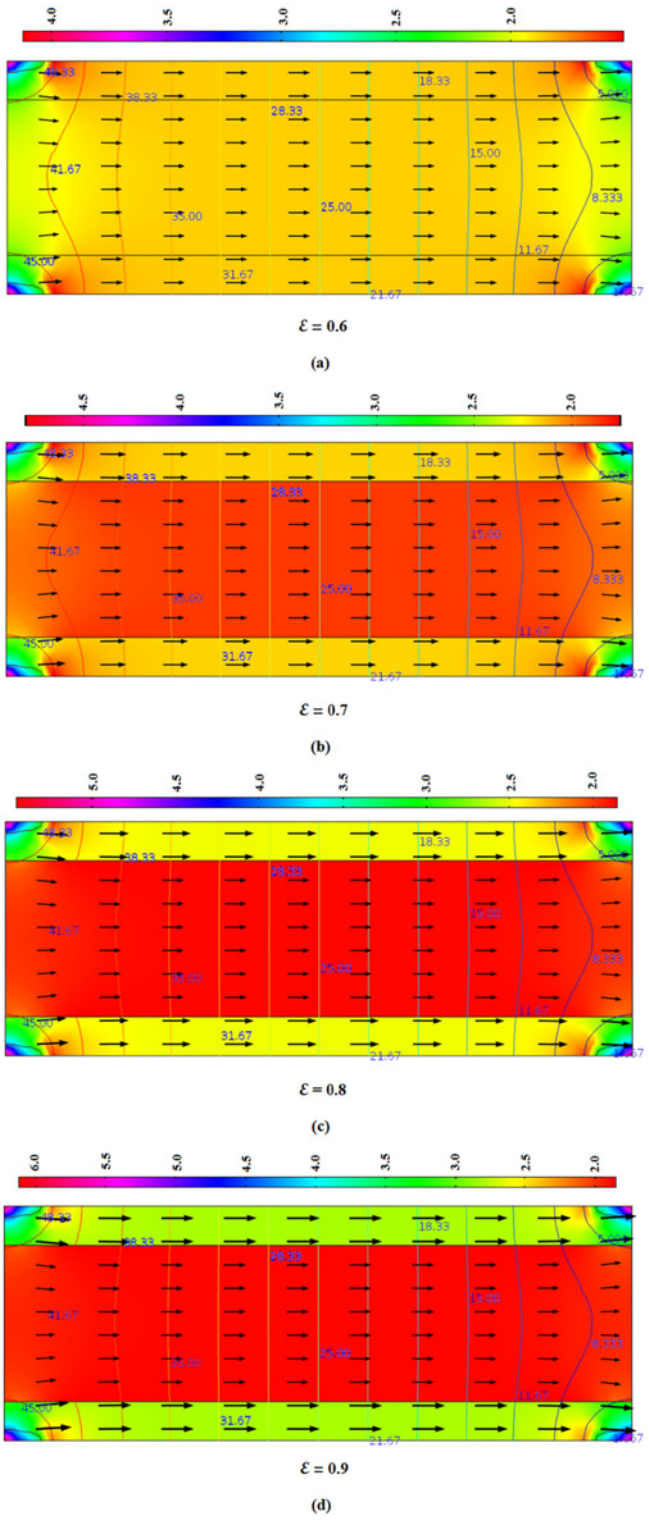

Fig. 3 Effect of composite porosity on pressure-driven velocity magnitude in mm/s (surface plot); voltage potential in V (contour plot) and flow velocity field (arrow plot) for (a) porosity = 0.6, (b) porosity = 0.7, (c) porosity = 0.8 and (d) porosity = 0.9

4.2 Effect on Pressure-driven Flow Velocity

Fig. 3 shows the surface plots for the pressure-driven velocity to compare the EOF velocity results on the composite porosity. Here, the arrow and contour plots represent flow velocity field and the voltage potential distribution, respectively. The effect of increased porosity near the wall region is more prominent in this case than EOF. The color gradient clearly shows the difference in velocity between two distinct regions, demonstrating the importance of the composite porosity phenomenon for the pressure-driven flows. An important feature that the EOF flow field lacks is the increase in flow rate in the central region in addition to the near wall region. This phenomenon reflects the strength of pressure-driven flows compared with EOF.

Fig. 4 shows the graphical plot for the EOF velocity magnitude at 2 mm from the inlet of the channel. A maximum difference of 0.27 mm/s was found in this case which is small when compared with a significant velocity difference of 1 mm/s for pressure-driven flows. The latter case also presents a slight variation in the velocity including in the central region, and which may become more prominent at a micro scale. The common feature of the two flow physics in the composite porous layer is the velocity gradient, which validates the model used in this study. Moreover, these effects may become more significant for improved boundary conditions of

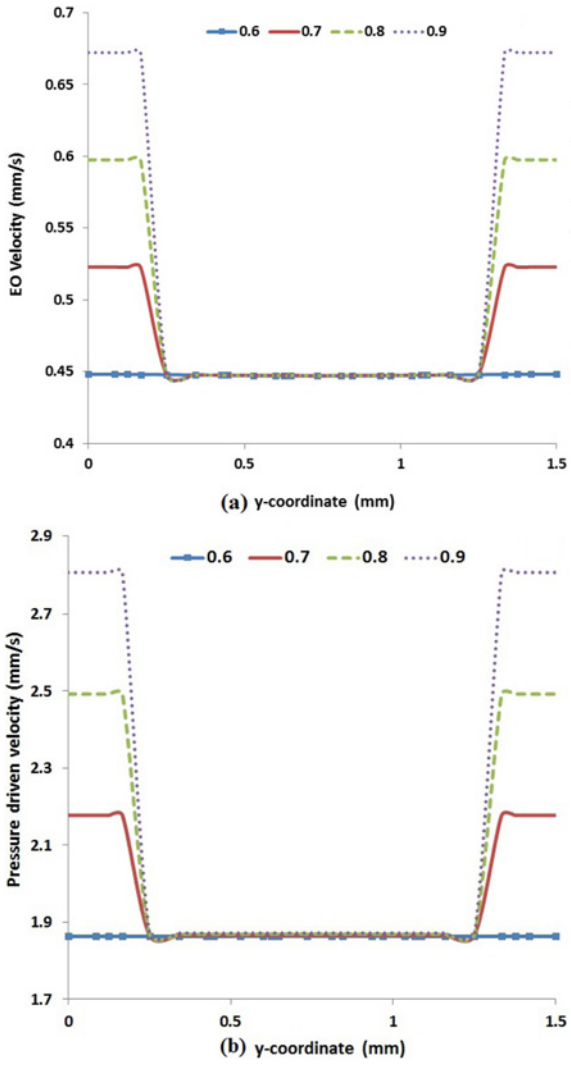

Fig. 4 Effect of composite porosity on: (a) electroosmotic velocity magnitude and (b) pressure driven velocity magnitude

high applied voltage and pressure. An interesting feature also exists in both flow types. The velocity at the interface of the two regions has a slight variation and is lesser than that in the constant porosity case. However, the velocity recovered quickly in the central region. Though the flow is strictly laminar in most of the domain; however, the velocity vectors tend to move across the interface of two distinct porous regions near the entrance and exit of the domain. This effect appears near the electrodes where a significant velocity gradient is observed.

4.3 Effect on Specie Mass Transport and Concentration Profile

Figs. 5 and 6 show the contour plots representing the transport of the tracer specie at four different times for the two combinations of constant porosity 0.6 and composite porosity of 0.8 in the outer region. Clearly, an increase in porosity increases the mass transport of the tracer. The composite porosity not only affects the concentration in the outer region but also the central region to some extent. This effect started early, and a part of the tracer in the outer region moved faster than that in the central region. Therefore, an increase in porosity improves the mass transport and compensates for the reduced porosity regions.

Fig. 7 shows the cross sections of the pulse along the interface of the two distinct porosity regions with different porosity near the wall region and the central region. Each graph represents the concentration profile for the following times: t = 0 s, t = 0.2 s, t = 0.4 s and t = 0.6 s. The mechanical diffusion of the tracer specie is responsible for the

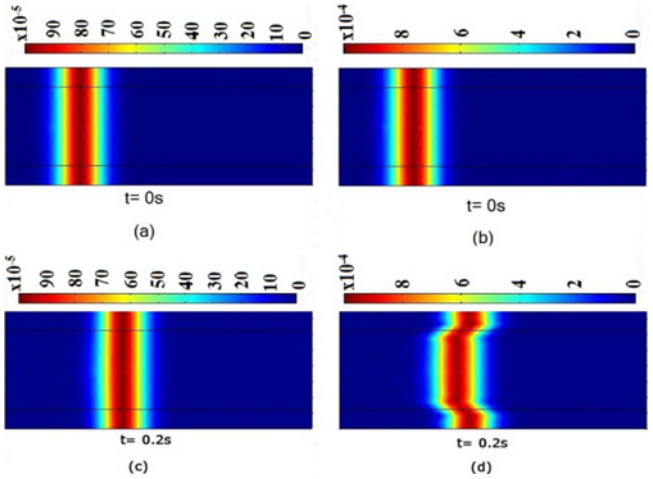

Fig. 5 Effect of composite porosity on tracer specie: (a) porosity = 0.6 and t = 0 s, (b) porosity = 0.8 and t = 0 s, (c) porosity = 0.6 and t = 0.2 s and (d) porosity = 0.8 and t = 0.2 s

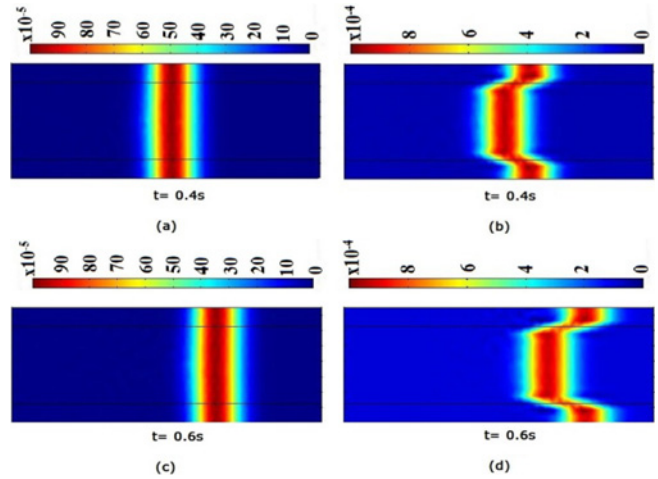

Fig. 6 Effect of composite porosity on tracer specie: (a) porosity = 0.6 and t = 0.4 s, (b) porosity = 0.8 and t = 0.4 s, (c) porosity = 0.6 and t = 0.6 s and (d) porosity = 0.8 and t = 0.6 s

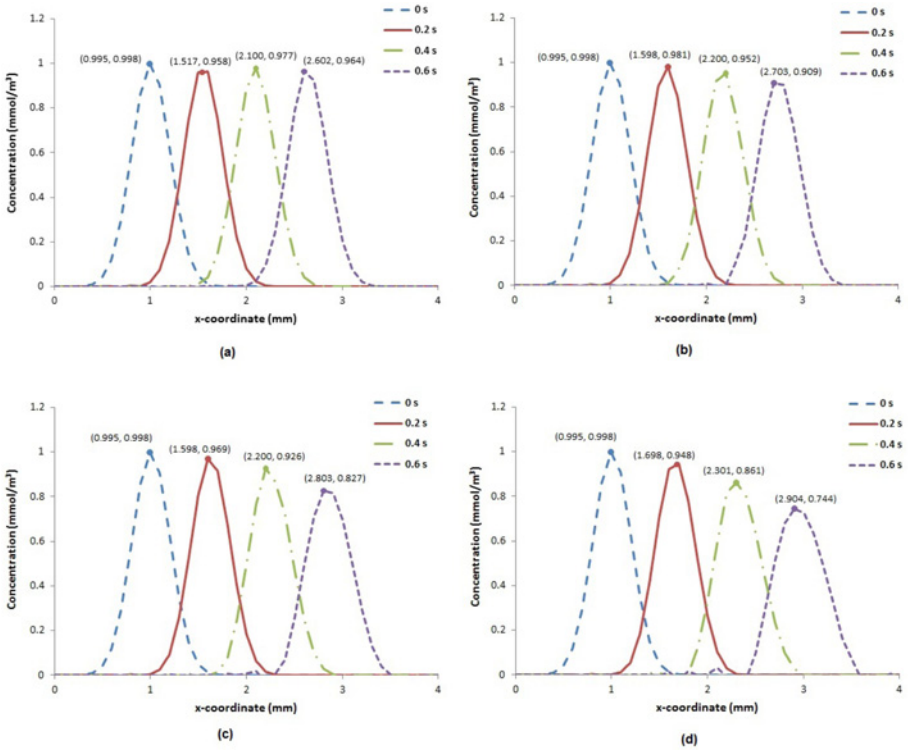

Fig. 7 Tracer concentration plots at composite porous interface (units: mmol/m^3); (a) porosity = 0.6, (b) porosity = 0.7, (c) porosity = 0.8 and (d) porosity = 0.9

generation of this pulse, whereas the pulse is translated and sheared by migration and convection. The uniform porosity in the two regions represents the same peak concentration for different times (Fig. 7(a)), whereas an increasing porosity near the wall region indicates the gradual reduction of peak concentration over time. These trends reflect the effect of composite porosity in the two regions (Fig. 7(b), (c), (d)). A concentration gradient at the interface was found at different times representing a strong porosity gradient. Thus, a relation between the two variables can be predicted with this result.

5. Conclusions

A numerical study addressing the issue of reduced porosity of porous layers because of the effect of solid boundary contact in EOF was carried out. This study emphasized the need for a composite porous layer with high porosity near the wall region. The results show an appreciable increase in velocity magnitude in the central region and near the wall region. This increase in velocity has also been prominently found in the case of pressure-driven flows.

The effects of composite porosity remain valid and significant for the mass transport of tracer specie in both regions, and a quicker mass transport was found in regions with high porosity, which will eventually compensate for the effect of the loss of porosity. Therefore, the authors propose the development of composite porous layers with a combination of different porosity value based on position in the porous domain to enhance the performance of devices such as an electroosmotic pump. Further detailed study considering the fluid structure interaction, viscous and shear effects of the fluid in porous media will provide more insight to the phenomenon of composite porosity and composite porous layers.

ACKNOWLEDGEMENT

This work was supported by a National Research Foundation of Korea (NRF) grant funded by the Korea Government (MEST) (No. 2012R1A2A2A01046099), and a grant from the Priority Research Centers Program through the National Research Foundation of Korea (NRF) funded by MEST (2012-0005856).

REFERENCES

1. Hunter, R. J., “Zeta Potential in Colloidal Science: Principles and Applications,” Academic Press, 1988.
2. Kozak, M. W. and Davis, E. J., “Electrokinetics of Concentrated Suspensions and Porous Media: I. Thin Electrical Double Layers,” Journal of Colloid and Interface Science, Vol. 127, No. 2, pp. 497-510, 1989.
3. Kozak, M. W. and Davis, E. J., “Electrokinetics of Concentrated Suspensions and Porous Media: II. Moderately Thick Electrical Double Layers,” Journal of Colloid and Interface Science, Vol. 129, No.1, pp. 166-174, 1989.
4. Rathore, A. S. and Horvath, C., “Capillary Electro Chromatography: Theories on Electroosmotic Flow in Porous Media,” Journal of Chromatography A, Vol. 781, No. 1, pp. 185-195, 1997.
5. Wang, M. and Chen, S., “Electroosmosis in Homogeneously Charged Micro and Nanoscale Random Porous Media,” Journal of Colloid and Interface Science, Vol. 314, No.1, pp. 264-273, 2007.
6. Yao, S. and Santiago, J. G., “Porous Glass Electroosmotic Pumps: Theory,” Journal of Colloid and Interface Science, Vol. 268, No. 1, pp. 133-142, 2003.
7. Buie, C. R., Posner, J. D., Fabian, T., Cha, S. W., Kim, D., et al., “Water Management in Proton Exchange Membrane Fuel Cells using Integrated Electroosmotic Pumping,” Journal of Power Sources, Vol. 161, No. 1, pp. 191-202, 2006.
8. Jiang, L., Michelson, J., Koo, J. M., Huber, D., Yao, S., et al., “Closed-loop Electroosmotic Microchannel Cooling System for VLSI Circuits,” IEEE Transactions on Components and Packaging Technologies, Vol. 25, No. 3, pp. 347-355, 2002.
9. Yao, S., Hertzog, D. E., Zeng, S., Mikkelsen, J. C., and Santiago, J. G., “Porous Glass Electroosmotic Pumps: Design and Experiments,” Journal of Colloid and Interface Science, Vol. 268, No. 1, pp. 143-153, 2003.
10. Chandrasekhara, B. C., Vortmeyer, D., and Miinchen, “Flow Model for Velocity Distribution in Fixed Porous Beds under Isothermal Conditions,” Thermo and Fluid Dynamics, Vol. 12, No. 2, pp. 105-111, 1979.
11. Vafai, K. and Tien, C. L., “Boundary and Inertia Effects on Flow and Heat Transfer in Porous Media,” International Journal of Heat and Mass Transfer, Vol. 24, No. 2, pp. 195-203, 1981.
12. Lee, H., Kim, G. M., Lee, C. Y., and Park, C. W., “Experimental Study on the Basic Performance of Electroosmotic Pump with Ion Exchanging Porous Glass Slit,” Intetnational Journal of Modern Physics B, Vol. 24, No. 15-16, pp. 2627-2632, 2010.
13. Ling, Z., Yang, T., Meng, F. C., Yi, L., and Zhang, X. X., “Simulation and Experimental Study of a Porous Electroosmotic Pump,” Key Engineering Materials, Vol. 483, pp. 320-326, 2011.
14. Roshendel, R., Farhanieh, B., and Iranizad, E. S., “The Effects of Porosity Distribution Variation on PEM Fuel Cell Performance,” Renewable Energy, Vol. 30, No. 10, pp. 1557-1572, 2005.
15. Roshandel, R. and Farhanieh, B., “The Effects of Non-uniform Distribution of Catalyst Loading on Polymer Electrolyte Membrane Fuel Cell Performance,” International Journal of Hydrogen Energy, Vol. 32, No. 17, pp. 4424-4437, 2007.
16. Iliev, O., Mikeli´c, A., and Popov, P., “On Upscaling Certain Flows in Deformable Porous Media,” Multiscale Modeling and Simulation, Vol. 7, No. 1, pp. 93-123, 2008.
17. Andrä, H., Iliev, O., Kabel1, M., Kirsch, R., Lakdawala, Z., et al., “Fluid-structure Interaction in Porous Media for Loaded Filter Pleats,” Proc. of the 82nd Annual Metting of the International

Association of Applied Mathematics and Mechanics, Vol. 11, No. 1, pp. 489-490, 2011.

18. Vafai, K., "Convective Flow and Heat Transfer in Variable-Porosity Media," Journal of Fluid Mechanics, Vol. 147, pp. 233-259, 1984.

19. Vafai, K., Alkire, R. L., and Tien, C. L., "An Experimental Investigation of Heat Transfer in Variable Porosity Media," Journal of Heat Transfer, Vol. 107, No. 3, pp. 642-647, 1985.

20. Lee, S. H., Lee, J. H., Park, C. W., Lee, C. Y., Kim, K., et al., "Continuous Fabrication of Bio-inspired Water Collecting Surface via Roll-type Photolithography," Int. J. Precis. Eng. Manuf.-Green Tech., Vol. 1, No.2, pp. 119-124, 2014.

21. Park, S. B. and Park, Y. I., "Fabrication of Gas Diffusion Layer Containing Microporous Layer using Fluorinated Ethylene Prophylene for Proton Exchange Membrane Fuel Cell," Int. J. Precis. Eng. Manuf., Vol. 13, No. 7, pp. 1145-1151, 2012.